Transient Infantile Hypertriglyceridemia, Fatty Liver, and Hepatic Fibrosis Caused by Mutated *GPD1*, Encoding Glycerol-3-Phosphate Dehydrogenase 1

Lina Basel-Vanagaite,[1,2,3,17,18,*] Noam Zevit,[2,4,18,*] Adi Har Zahav,[2] Liang Guo,[5,6,7] Saj Parathath,[5,6,7] Metsada Pasmanik-Chor,[8] Adam D. McIntyre,[9,10] Jian Wang,[9,10] Adi Albin-Kaplanski,[11] Corina Hartman,[2,4] Daphna Marom,[2,12] Avraham Zeharia,[2,13] Abir Badir,[14] Oded Shoerman,[2,15] Amos J. Simon,[16] Gideon Rechavi,[2,16] Mordechai Shohat,[2,3,17] Robert A. Hegele,[9,10] Edward A. Fisher,[5,6,7] and Raanan Shamir[2,4]

The molecular basis for primary hereditary hypertriglyceridemia has been identified in fewer than 5% of cases. Investigation of monogenic dyslipidemias has the potential to expose key metabolic pathways. We describe a hitherto unreported disease in ten individuals manifesting as moderate to severe transient childhood hypertriglyceridemia and fatty liver followed by hepatic fibrosis and the identification of the mutated gene responsible for this condition. We performed SNP array-based homozygosity mapping and found a single large continuous segment of homozygosity on chromosomal region 12q13.12. The candidate region contained 35 genes that are listed in Online Mendelian Inheritance in Man (OMIM) and 27 other genes. We performed candidate gene sequencing and screened both clinically affected individuals (children and adults with hypertriglyceridemia) and also a healthy cohort for mutations in *GPD1*, which encodes glycerol-3-phosphate dehydrogenase 1. Mutation analysis revealed a homozygous splicing mutation, c.361−1G>C, which resulted in an aberrantly spliced mRNA in the ten affected individuals. This mutation is predicted to result in a truncated protein lacking essential conserved residues, including a functional site responsible for initial substrate recognition. Functional consequences of the mutation were evaluated by measuring intracellular concentrations of cholesterol and triglyceride as well as triglyceride secretion in HepG2 (hepatocellular carcinoma) human cells lines overexpressing normal and mutant *GPD1* cDNA. Overexpression of mutant *GPD1* in HepG2 cells, in comparison to overexpression of wild-type *GPD1*, resulted in increased secretion of triglycerides ($p = 0.01$). This finding supports the pathogenicity of the identified mutation.

Introduction

The two main sources of plasma triglycerides (TG) are exogenous TG, absorbed in the gut and transported into the plasma as chylomicrons, and endogenous TG, synthesized in the liver and secreted as part of very-low-density lipoprotein (VLDL) particles.[1] Elevated TG levels may represent primary hereditary disorders[2,3] or be secondary to other conditions, particularly obesity and type 2 diabetes mellitus.[4–9] A molecular basis for primary hypertriglyceridemia has been identified in fewer than 5% of cases.[10] The study of monogenic dyslipidemias has the potential to expose key pathways previously unrecognized in lipid metabolism. An example includes autosomal-dominant familial hypercholesterolemia [MIM 143890], whose characterization led to the discovery of receptor-mediated endocytosis via the low-density lipoprotein receptor, paving the way to the development of statins.

Severe monogenic hypertriglyceridemia can be seen with fasting chylomicronemia caused by complete lipoprotein lipase deficiency [MIM 238600] or from apo CII deficiency [MIM 207750] or without fasting chylomicronemia, including partial lipoprotein lipase deficiency, dysbetalipoproteinemia type III or hepatic lipase deficiency [MIM 151670], and collagen 18 deficiency [MIM 267750].[11] Elevations of plasma TG-rich lipoproteins result from either increased production in the liver or decreased TG uptake. High TG levels are often associated with elevated cholesterol levels leading to accelerated formation

[1]Department of Pediatric Genetics, Schneider Children's Medical Center of Israel, 14 Kaplan Street, Petah Tikva 49202, Israel; [2]Sackler Faculty of Medicine, Tel Aviv University, Tel Aviv 69978, Israel; [3]Raphael Recanati Genetic Institute, Rabin Medical Center, Beilinson Hospital, Petah Tikva 49100, Israel; [4]Institute of Gastroenterology, Nutrition, and Liver Diseases, Schneider Children's Medical Center of Israel, 14 Kaplan Street, Petah Tikva 49202, Israel; [5]Department of Medicine, New York University School of Medicine, New York, NY 10016, USA; [6]Leon H. Charney Division of Cardiology, New York University School of Medicine, New York, NY 10016, USA; [7]Marc and Ruti Bell Vascular Biology and Disease Program, New York University School of Medicine, New York, NY 10016, USA; [8]Bioinformatics Unit, George S. Wise Faculty of Life Sciences, Tel Aviv University, Tel Aviv 69978, Israel; [9]Robarts Research Institute, University of Western Ontario, London, Ontario N6A 5K8, Canada; [10]Schulich School of Medicine and Dentistry, University of Western Ontario, London, Ontario N6A 5K8, Canada; [11]Tissue Typing Laboratory, Rabin Medical Center, Beilinson Hospital, Petah Tikva 49100, Israel; [12]Department of Pediatrics A, Schneider Children's Medical Center of Israel, 14 Kaplan Street, Petah Tikva 49202, Israel; [13]Day Clinic, Schneider Children's Medical Center of Israel, 14 Kaplan Street, Petah Tikva 49202, Israel; [14]Clalit Health Services, Kfar Kasem 48810, Israel; [15]Department of Pediatrics B, Schneider Children's Medical Center of Israel, 14 Kaplan Street, Petah Tikva 49202, Israel; [16]Sheba Cancer Research Center, The Chaim Sheba Medical Center, Tel Hashomer 52621, Israel; [17]Felsenstein Medical Research Center, School of Medicine, Tel Aviv University, Rabin Medical Center, Beilinson Campus, Petah Tikva 49100, Israel, associated with
[18]These authors contributed equally to this work
*Correspondence: basel@post.tau.ac.il (L.B.-V.), nzevit@gmail.com (N.Z.)
DOI 10.1016/j.ajhg.2011.11.028.

of atherosclerotic plaques.[12–14] Furthermore, several studies indicate that hypertriglyceridemia is an independent risk factor for coronary artery disease.[14–18] Extreme hypertriglyceridemia is also associated with an increased risk of acute pancreatitis.[19]

Frequently, novel genetic diseases occur in families with a high degree of consanguinity because this increases the likelihood of identical-by-descent pathogenic mutations as a result of inheritance from a common ancestor. Thus, homozygosity mapping has become the most robust strategy for the discovery of new genetic variants. In this study we describe a hitherto unreported form of autosomal-recessive moderate to severe transient hypertriglyceridemia in infancy and early childhood that is associated with hepatic steatosis and the development of fibrosis. Using homozygosity mapping, we identified a disease-causing mutation, c.361−1G>C [p.Ile119fsX94]), in *GPD1* (MIM 138420), which encodes glycerol-3-phosphate dehydrogenase 1 (GPD1).

Subjects and Methods

Affected Individuals

We identified four Israeli Arab families with a total of ten affected family members (Figure 1A). In each of these families, there were instances of both consanguineous and nonconsanguineous marriages; however, all the families originate from the same isolated population within a single village with a very high rate of consanguinity. All the affected children presented in infancy with similar clinical symptoms of the disease. We obtained informed consent from all family members or their legal guardians according to a protocol approved and reviewed by the Helsinki committee of the Rabin Medical Center and in accordance with a protocol approved and reviewed by the National Committee for Genetic Studies, Israeli Ministry of Health.

For comparison, a group of white Canadian children (n = 16, age range 1 month to 18 years) with severe hypertriglyceridemia, 75 white adults with severe hypertriglyceridemia who had no mutations in known genes, and 47 matched normolipidemic Canadian controls were evaluated for sequence changes in *GPD1*.

The project had the approval of the office of research ethics, University of Western Ontario, review number 07920E.

Homozygosity Mapping and Linkage Analysis

Genomic DNA for genotyping was extracted from peripheral blood leukocytes in EDTA by standard procedures. SNP genotyping was performed on Affymetrix Human Mapping 250k NspI arrays (Affymetrix, Santa Clara, CA, USA). All procedures and methods were performed according to the manufacturers' protocols. The mapping data were analyzed with the Homozygosity Mapper program.[20]

Sequencing of *GPD1*

Sequencing of the candidate gene was performed with primer sets designed with the Primer3 program. All exons, including exon-intron junctions, 5′ UTRs, and 3′ UTRs, were amplified from genomic DNA with primers designed from the genomic sequences available from the University of California-Santa Cruz (UCSC) Genome Browser (assembly hg19). Both strands of the PCR products were sequenced with BigDye Terminators on an ABI 3100 sequencer (Applied Biosystems, Foster City, USA). Sequence chromatograms were analyzed with SeqScape software version 1.1 (Applied Biosystems). We initially sequenced the gene from one affected individual and one heterozygous parent. Sequencing of genomic *GPD1* (NC_000012.11) was performed with eight primer pairs (Table S1, available online). *GPD1* mutation screening was performed on genomic DNA by PCR amplification with primer 4F, 5′-ACTT GAGCTGGGTTGGAATG-3′ (forward), and primer 4R, 5′- GAGA TGGCTAAGTGGGGTTG-3′ (reverse), followed by sequencing.

GPD1 Mutation Detection by Restriction Analysis

Amplification of a 362 bp fragment from genomic DNA was performed with primers GPD1-4F and 4R for nine cycles at an annealing temperature of 64°C and 26 cycles at an annealing temperature of 55°C. The mutation eliminates a DdeI restriction site that digests the 362 bp fragment into 11, 119, and 232 bp pieces, compared to a control sample, which digests into 11, 17, 119, and 215 bp pieces. The fragment was digested with 2 U/μg DdeI (New England Biolabs, Ipswich, MA, USA), and the products were separated on 3% NuSieve/ 1% agarose gels.

Sequencing of *GPD1* in Children and Adults with Hypertriglyceridemia and Controls

The 16 Canadian children (described above) with severe hypertriglyceridemia (plasma TG range 1592-11,504 mg/dl [18 to 130 mmol/L]) were evaluated. In these individuals, previous Sanger sequencing showed no mutations in *LPL* or *APOC2*, which encode lipoprotein lipase and apolipoprotein C-II, respectively. We also evaluated from a previously reported cohort[21] 75 white adults with severe hypertriglyceridemia (mean plasma TG 1,239 mg/dl [14.0 mmol/L]) who had no mutations in known genes, and 47 matched normolipidemic controls (mean plasma TG 97 mg/dl [1.1 mmol/L]). Bidirectional Sanger sequencing of *GPD1* coding regions and intron-exon boundaries on genomic DNA was performed with the same primers on a model 3730 Automated DNA Sequencer (Applied Biosystems, Mississauga, ON) at the London Regional Genomics Centre (London, ON).

Bioinformatics Methods and Servers

GPD1 was described with the UCSC (February 2009 [GRCh37/hg19]), NCBI (Build 37.1 [August 2009]) and Ensembl (February 2009 [GRCh37]) genome browsers. Evolutionary conserved regions (ECR) browser analysis was performed on Human genome (hg18) in order to show *GPD1* genomic conservation.[22] Pairwise alignments were performed between human and various species, including fugu pufferfish ([*Takifugu rubripes*], fr2), spotted green pufferfish ([*Tetraodon nigrovoridis*] tetNig1), frog ([*Xenopus laevis*] xenTro), chicken ([Gallus gallus] galGal), mouse ([*Mus musculus*] mm9), rat ([Rattus norvegicus] rn4), dog ([Canis familiaris] canFam), rhesus monkey ([Macaca mulatta] rheMac) and chimpanzee ([Pan troglodytes] panTro2).[22] Structure information was obtained from the PDBSum server,[23] based on the crystal structure of GPD1.[24] Domain properties for GPD1 were obtained from UniProt server, Pfam database (PF) version 24.0 (10/2009),[25] and InterPro server (IPR).[26] Information on protein expression was extracted from the Bgee database.[27]

Plasmid Construction

RNA was extracted from the affected individual's lymphoblastoid cell line with Trizol reagent (Invitrogen Life Technologies,

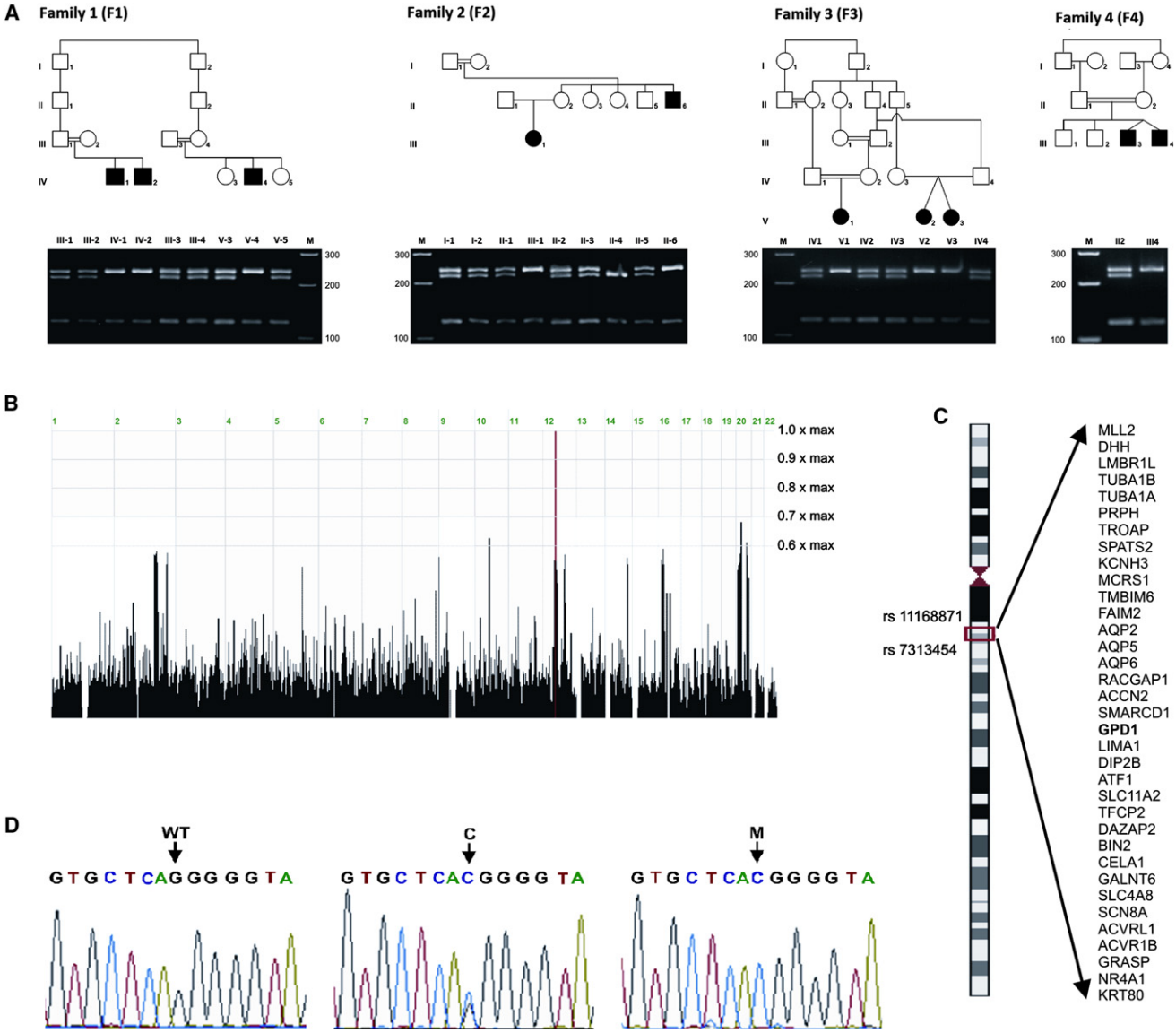

Figure 1. Family Tree, Candidate Region, and Mutation Analysis
(A) Pedigrees of the families and segregation analysis of the mutation. Segregation was assayed by PCR amplification of the genomic DNA and restriction by DdeI. The mutation eliminates a DdeI restriction site, which digests the 362 bp fragment into 11, 119, and 232 bp fragments, compared to a control sample, which digests into 11, 17, 119, and 215 bp. Blackened symbols represent affected individuals.
(B) Homozygosity region as defined by Homozygosity Mapper. Red lines represent the homozygosity region common to individuals F2-III1 and F1-IV4.
(C) Candidate region (only OMIM genes listed).
(D) Mutation analysis of *GPD1*. Sequence chromatogram from wild-type (WT), carrier (C), and affected (M) genotypes on genomic DNA and cDNA.

Carlsbad, CA, USA) according to the manufacturer's instructions. Complementary DNA (cDNA) was synthesized with a High Capacity cDNA Reverse Transcription Kit (Applied Biosystems), according to the manufacturer's protocol. The wild-type human *GPD1* was cloned from a pDrive-hGPD1 full-length cDNA clone (Openbiosystems, Huntsville, AL, USA) into pcDNA3.1 plasmids with HindIII and XhoI sites. The mutated cDNA was amplified with primers introducing the BamHI and NotI restriction sites, respectively (underlined): forward: 5′-GAGGATCCACCATGGCT AGCAAGAAAG-3′; reverse: 5′-GCGCGGCCGCTCAGTGACCAGT CACTGCT-3′. The amplified fragment was digested with the BamHI and NotI enzymes and subsequently ligated into pcDNA3 plasmids, digested with the same enzymes, with T4 ligase (Promega, Madison, WI). The integrity of the plasmid sequence was verified with direct DNA sequencing.

Normal and Mutant cDNA Transfection and Expression in HepG2 Cells

To simulate the homozygous recessive state in vivo, we overexpressed mutant *GPD1* cDNA in HegG2 cells, which presumably results in the majority of *GPD1* molecules being in the form expressed in the affected individuals. HepG2 cells were cultured in Dulbecco's modified Eagle's medium (DMEM) (Cellgro Mediatech, Manassas, VA, USA) with 10% FBS, 1 mM L-glutamine

Table 1. Clinical Characteristics of the Affected Individuals

	F1-IV1	F1-IV2	F1-IV4	F2-II6	F2-III1	F3-V1	F3-V2	F3-V3	F4-II4	F4-III3
Birth (week)	NA	NA	36	NA	40	42	37[a]	37[a]	34[a]	34[a]
Birth weight (grams)	3,000	NA	2,180	3,395	2,570	3,000	2,430	2,190	1,950	2,160
Presenting signs and symptoms	V	HM, V	HM	HM	HM, FTT	HM, V	HM	HM	HM	LFT
Presenting age (months)	1	1	4–6	Birth	6	2.5	7	7	9	3.5
Liver size at presentation (cm)	NA	NA	6–7 BCM	6–7 BCM	12 S	4 BCM	8 BCM	10 BCM	7 BCM	4[b] BCM
Spleen at presentation (cm) BCM	NA	NA	0	3	NA	0	2	4–5	0	0
Age at last exam (years)	14.2	9.8	11.9	23	2.9	4.3	1.3	1.3	12.2	11
Height (cm) at last exam (SDS)	161 (−0.50)	127 (−1.65)	126.5 (−3.05)	160 (−2.34)	84.5 (−1.94)	100 (−0.59)	77 (−0.30)	74 (−1.25)	130.8 (−2.70)	129 (−2.13)
Weight at last exam (SDS)	65.5 (1.14)	22.5 (−2.28)	25.8 (−2.66)	58.5 (−0.93)	12.3 (−0.75)	16.5 (0.06)	9.3 (−1.16)	8.2 (−2.44)	26.5 (−2.75)	25.6 (−2.14)
Liver at last exam (cm)	4 S	5 S	12 S	15 S	13 S	3–4 BCM	9.5 S	11 S	NA	NA

The following abbreviations are used: BCM, below costal margin; FTT, failure to thrive ; HM, hepatomegaly; LFT, elevated liver enzymes; NA, not available; S, span; SDS, standard deviation score; Centers for Disease Control (CDC) 2000 (see Web Resources); V, vomiting.
[a] Twin.
[b] At 1.5 years of age.

and 1% pen/strep and incubated at 37°C in a 5% CO_2 incubator. The cells were transiently transfected with pcDNA3.1-hGPD1 wild-type or pcDNA3.1-hGPD1 mutant constructs in Opti-MEM (Invitrogen, Camarillo, CA, USA) with FuGENE HD Transfection Reagent (Roche, Indianapolis, IN, USA), according to the manufacturer's protocol. Forty-eight hours after transfection, cellular lipids were extracted and total cholesterol and TG were quantified enzymatically with Cholesterol E and L-Type TG M kits (Wako Diagnostics, Richmond, VA, USA). For measurement of the TG secretion, HepG2 cells were washed twice with cold PBS and incubated with serum-free medium for 6 hr. The concentration of the secreted TG in the medium was quantified fluorometrically at Ex/Em 530 nm/590 nm with a TG quantification kit (BioVision, Mountain View, CA, USA). The results were normalized to the total protein, which was measured with the Bio-Rad Dc protein assay.

Results

Clinical and Laboratory Evaluation

All of the affected individuals presented between the ages of 1 and 9 months. Their clinical characteristics are shown in Table 1. The presenting complaints included vomiting (n = 3), poor weight gain (n = 1), and asymptomatic (n = 6). On initial examination they had moderately to severely enlarged livers, and three had mild to moderate splenomegaly. Fasting hypertriglyceridemia was universally present, ranging from mild to severe (TG 258–6,244 mg/dl [2.91–70.6 mmol/l] normal 50–150 mg/dl), as were elevated transaminases and gamma-glutamyl transferase (GGT). Bilirubin and synthetic liver function (coagulation studies and albumin) were within normal limits at presentation and throughout the follow-up period (Table 2). Cholesterol levels were normal in all but one of the infants (whose levels normalized during follow-up). Of note, all of those in whom liver enzymes (F1-IV4, F4-III3, F4-II4) and TG (F1-IV4) were examined at birth had normal levels and a liver with a normal span. Sonographic findings compatible with fatty liver were present in eight of the ten affected individuals at presentation, and the remaining two developed similar findings at 1 year of age. These included diffuse hyperechogenicity of the liver parenchyma with a fine granular pattern and, in some affected individuals, loss of portal spaces (Figures 2E–2F). None have yet developed cutaneous xanthomas. Fasting hypoglycemia was not present. Individual F4-III3 has the additional diagnoses of infantile intraventricular hemorrhage, transverse sagittal sinus thromboses, decreased protein C, celiac disease, epilepsy, acquired microcephaly, and communicating hydrocephalus with a ventriculo-peritoneal shunt. At the time of his hemorrhage, he had episodes of severe hyperglycemia (over 1,000 mg/dl), which did not recur at other times of stress or illness. In addition, he had mildly and intermittently elevated pyruvic acid and moderate elevations of ammonia. This affected individual is the twin of affected individual F4-II4, who has a horseshoe kidney, and they have another sibling who has the CHARGE association (coloboma, heart defects, atrasia choanae, retarded growth/development, genital,

Table 2. Laboratory Testing Results

Affected Individual	Age at Initial Tests (Months)	Age at Last Tests (Years)	Initial TG[a] (mg/dl)	Last TG[a] (mg/dl)	Initial Cholesterol (mg/dl)	Last Cholesterol (mg/dl)	Initial ALT (U/l)	Last ALT (U/l)
F1-IV1	1	13.7	**6,244**	**250**	**420**	73	**230**	39
F1-IV2	1	9.9	**250**	**247**	109	**207**	**115**	**81**
F1-IV4	6	11.9	**990**	**289**	164	172	**83**	37
F2-II6	0.25	23	**520**	170	101	114	**109**	**79**
F2-III1	6	2.9	**1,208**	**202**	109	184	**125**	**70**
F3-V1	2.5	4.3	**349**	135	66	**202**	**155**	29
F3-V2	7	1.3	**258**	185	95	118	**51**	**38**
F3-V3	7	1.3	**330**	**202**	99	141	**94**	**71**
F4-II4	9	12.5	**225**	**301**	106	188	**132**	**93**
F4-III3	3.5	12.5	**566**	**434**	149	**256**	**90**	**165**

Values in bold are elevated beyond normal values for age. 1 mg/dl TG = 0.0113 mmol/l (normal 10–150 mg/dl); 1mg/dl cholesterol = 0.0259 mmol/l (normal < 170 mg/dl, borderline 170–200 mg/dl). Normal ALT 7–50 U/l up to 6 months and 7–35U/l beyond 6 months.
[a] Fasting TG levels.

ear abnormalities). Besides this individual and one other who had transient hypotonia of infancy that later resolved, all others had normal neurologic findings throughout their follow-up including muscle tonus and motor development, and all have physical capabilities compatible with their respective ages.

In-depth studies were performed. These produced normal results and included infectious serologies (hepatitis A, B, and C viruses, Epstein-Barr virus [EBV], cytomegalovirus [CMV], human immunodeficiency virus [HIV] [three examined], toxoplasma [five examined]), thyroid studies, alpha-1 anti-trypsin levels, galactose 1 phosphate uridyl transferase activity, serum amino acids, ferritin, creatine phosphokinase, alpha-fetoprotein (high in one individual at 3 months, normalized at 3 years), albumin, smooth-muscle antibody, anti liver-kidney microsomal antibody, nuclear antibody (elevated in one affected individual), mitochondrial antibody, sweat test, vertebral X-rays, immunoglobulin levels, and glycogen storage diseases 3 and 6. Apolipoproteins A1, B, C2, and C3 levels, and apo E genotype were measured in six affected individuals. The samples were drawn in all but one affected individual when TG levels were either normal or only mildly elevated (after the *GPD1* mutation was identified). In the individual with severely elevated TG (1,250 mg/dl), apo C2 and apo C3 were elevated to 12.2 and 42.2 mg/dl, respectively (normal apo C2, 3–7 mg/dl; apo C3 9–19 mg/dl). One individual with mild hypertriglyceridemia (293 mg/dl) had elevated apo C3 (25 mg/dl), and one affected individual with normal TG (163 mg/dl) had low levels of apo C2 (1.8 mg/dl) and apo C3 (7.0 mg/dl). High-density lipoprotein-calculated levels were, not surprisingly, low at early ages and increased to normal levels over time. Interestingly, five of nine affected individuals for whom urinary organic acid profiles were available had mildly elevated fasting urinary dicarboxylic acids with a nonspecific pattern. Of these, two had elevated and two decreased ketones. Dicarboxylic aciduria decreased as the affected individuals' age increased. Lactate levels were normal, pyruvate was borderline in three, and ammonia elevated only in individual F4-III3, who had several additional diagnoses, as described above. In order to further investigate a possible derangement of beta-oxidation or a more general mitochondrial or peroxisomal disorder, acyl-carnitine profiles and free fatty acids were measured in six affected individuals and very-long-chain fatty acids in five. All were found to be normal.

Although transaminases normalized in four, the majority had elevated liver enzymes at the time of their last clinical evaluation. Triglyceride levels decreased in eight individuals; however, in seven the levels were still above 200 mg/dl. Total cholesterol levels increased moderately in nine individuals, but remained within normal limits in all but three (Table 2). The oldest affected individual, F2-II6, 23 years of age at the last follow-up, remains asymptomatic, with short stature, elevated transaminases, and a hyperechoic liver compatible with fatty change. None of the heterozygous parents or siblings examined had elevated TG or transaminases except for one morbidly obese mother who had elevated triglycerides without findings compatible with hepatic steatosis on ultrasound. The heterozygous mother of affected individual F2-II6 (grandmother of affected individual F2-III1) had a mild fatty liver on ultrasound at 47 years of age and normal liver function tests. One family had a history of early cardiovascular disease.

Two individuals, F1-IV4 and F1-IV2, underwent liver biopsies at 4.5 and 2.5 years, respectively. The biopsies demonstrated marked mixed macro- and microsteatosis with fibrosis and septal formation. Both had mild inflammatory infiltrates; in one there was a mixed infiltrate, whereas in the other it was mononuclear (Figure 2). Four

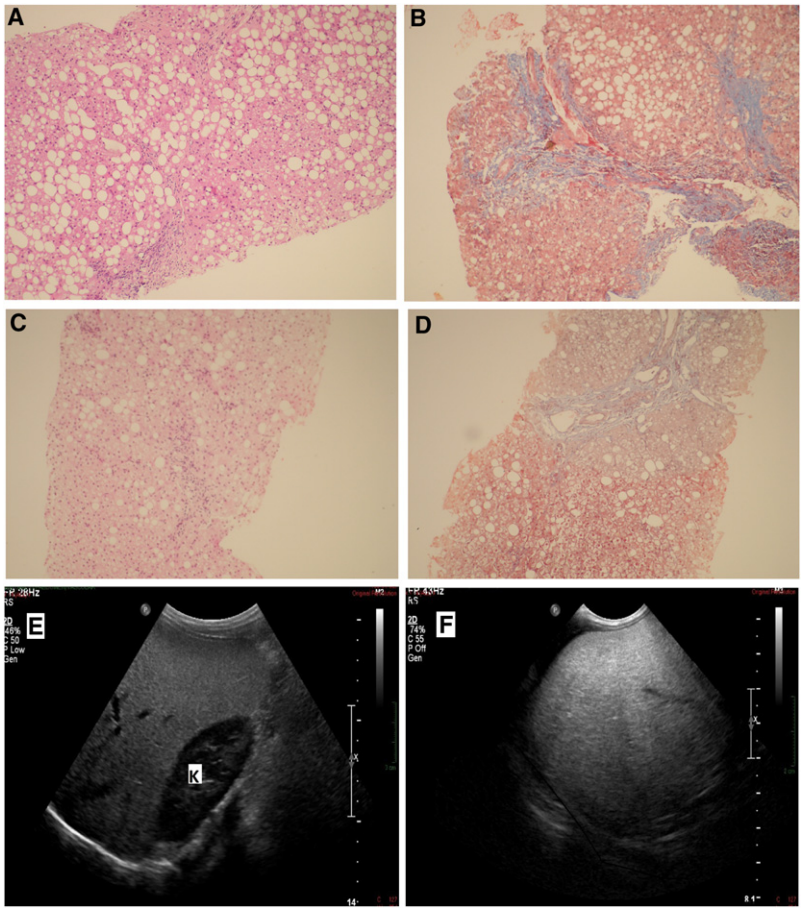

Figure 2. Liver Biopsies and Ultrasound
(A and B) Affected individuals F1-IV2 at 2.4 years of age: Trucut liver biopsy. (A) The liver parenchyma shows macro- and microvesicular fatty change and mild mononuclear inflammatory infiltrate in the portal spaces. Hematoxylin and eosin staining (H&E), magnification 10×. (B) Widening of the portal spaces because of fibrotic deposition with septal formation. Masson trichrome stain, magnification 10×.
(C and D) Affected individual F1-IV4 at 4.5 years of age: Trucut liver biopsy. (C) Liver parenchyma shows fatty change, both macro- and microvesicular, and small collections of inflammatory cells, including lymphocytes, histiocytes, polymorphonuclears, and eosinophils. H&E, magnification 10×. (D) Portal fibrosis with septal formation and mild sinusoidal fibrosis. Masson Trichrome stain, magnification 10×.
(E) Ultrasound of affected individual F1-IV4 at 11.9 years of age demonstrates diffuse hyperechogenicity of the liver with a fine granular pattern. In comparison, the kidney parenchyma (K) appears hypoechoic.
(F) Ultrasound of another affected individual at 3 months of age showing dense diffuse hyperechogenicity of the liver with loss of imaging of the portal areas.

affected individuals have short stature (height standard deviation score < -2 standard deviation).

Mapping of the Candidate Region to 12q13.12

Visual inspection of the SNP data and homozygosity analysis with Homozygosity Mapper showed that the two affected individuals initially examined, F2-III1 and F1-IV4, exhibited a single large continuous segment of homozygosity on 12q13.12 for 163 consecutive SNPs between markers rs11168871 and rs7313454, encompassing 2.9 Mb (Figure 1B). These data were supportive of homozygosity by descent. There were no additional significant regions of homozygosity. The candidate region contained 35 genes that are listed in Online Mendelian Inheritance in Man (OMIM) and 27 other genes (Figure 1C).

Mutation Analysis

Because *GPD1* is known to be associated with glycerol metabolism, it was prioritized as a candidate for sequencing because we thought it was the most likely gene to be mutated in the affected children.

Sequencing of *GPD1* revealed a splice-site mutation in intron 3, c.361−1G>C, at coding sequence position 360 (NM_005276.2, according to Recommendations for the Description of DNA Sequence Variants [Ensembl Genome Browser]) (Figure 1D). The normal transcript is composed of eight coding exons. The resulting mutated transcript is predicted to consist of the first three exons (360 bps, 120 amino acids) and an addition of 279 bps (93 amino acids) translated from intron 3, creating a mutated protein of 213 residues: c.361−1G>C (p.Ile119fsX94) (ss472336569) (Figure 3). The mutation segregates with the disease; affected individuals displayed homozygous mutations, whereas parents displayed heterozygosity for a normal and a disease allele, consistent with autosomal-recessive inheritance (Figure 1A). The mutation was not observed in 404 chromosomes from unrelated control individuals of Arab origin and 94 chromosomes of non-Arab origin.

Bioinformatics Analysis

Pairwise alignments are shown between human and various species as described in the methods section (Figure 4). The human and chimpanzee proteins are identical (99% at the nucleotide level), whereas the mouse protein shared 96% identity to human (NCBI UniGene Hs.524418). Human *GPD1* resides within chromosomal region 12q12-q13 (50,497,801–50,505,096; 7,296 bps; RefSeq: NM_005276.2). The mRNA consists of 2,909 bps, including eight exons, all coding. The open reading frame size is 1,050 bps encoding a protein of 349 residues (NP_005267.2; P21695; GPDA_HUMAN), (Uniprot database) (Figures 4B and 4C). GPD1 consists of two domains: NAD_Gly3P_dh_N (PF01210; IPR011128) and NAD_Gly3P_dh_C (PF07479; IPR006109) (Figure 4C). The *Homo sapiens* GPD1 (Enzyme Commission numberEC

GPD1 Mutant cDNA

gcactgagccggctcaggcagagacgcggcaccATGgctagcaagaaagtctgcattgtaggctccgggaactggg
gctcagccatcgccaagatcgtgggtggcaatgcagcccagctggcacagtttgacccacgggtgaccatgtgggtattt
gaggaagacattggaggcaaaaagctgactgagatcatcaacacgcagcatgagaatgtcaaatacctgccagggcac
aagttgccccccaaatgtggtggctgtcccagatgtggtccaggctgcagaggatgctgacatcctgatctttgtggtgccc
catcagttcatcggcaagatctgtgaccagctcaagggccatctgaaggcaaacgccactggcatatctcttattaaggtg
ccagggacaccttcatgtggatgggggagggtgcggctcactgttgtggggttcagggtgggtgaagcaaggagaaca
gaaaatggcagacgcaggccaagagtttgctggagaaaagagaggcagttggctctggagaggcttaggaaagcagt
gaggtgctgggggtcactggaagggaggctgaagggaggagacgagattggtttggaggtcctctcggggagtttcgg
aggtataaaggaatgcctgggagatatgagaagcgggctggttTGAgaagtgtgaagagtagctggtttggagcagt
gactggtcactgaatggcagtttgttggggcagtcaggcgg

Exon1 Exon2 Exon3 Intron3

Figure 3. cDNA Analysis of Splice-Site Modification in an Affected Individual and Control
Splice-site mutation eliminating the exon 4 splice site and creating a shorter protein by translation continuation from the mutation site until a stop codon in-frame.

1.1.1.8) belongs to the NAD-dependent glycerol-3-phosphate dehydrogenase family; it is soluble and is found in the cytoplasm. The protein has been cloned from the human liver.[28] GPD1 catalyzes the reversible redox reaction of dihydroxyacetone phosphate (DHAP) and nicotine adenine dinucleotide, reduced (NADH) to glycerol-3-phosphate (G3P) and nicotinamide adenine dinucleotide (NAD^+) and together with a mitochondrial enzyme, glycerol-3 phosphate dehydrogenase 2 (GPD2), plays an important role in the transport of reducing equivalents from the cytosol to the mitochondria. The crystal structure of GPD1 has been delineated;[24] it shows a secondary structure with various active sites in addition to a relatively conserved C terminal (Figure 4B). The key residue for initial recognition of the substrate (Arg269) has been identified.[24] *GPD1* is expressed in a variety of tissues, including various regions of the brain, internal tissues, and many other tissues and is found in all the human developmental stages (Bgee database).[27] In pigs, mesentery fat, subcutaneous fat, and duodenum demonstrate the highest levels of expression of *GPD1*; liver, kidney, cerebellum, ileum, and latissimus dorsi muscle have intermediate levels, whereas the heart, pancreas, spleen, jejunum, and cerebrum exhibit the lowest levels.[29] The mutated protein is predicted to be truncated, missing section of the protein containing essential components, including major secondary structures and essential conserved residues, some of them known as active sites (Figure 4B).[24] Moreover, the mutated protein has acquired 93 new amino acids that do not show any ordered domains.

Evaluation of Children and Adults with Hypertriglyceridemia

Several common and rare variants of *GPD1*, both synonymous and nonsynonymous, were found in both cases and controls from the Canadian cohort (Table 3). Most of these have been previously reported in normal populations. No variant differed in frequency between cases and controls.

Evaluation of the Functional Consequences of the Mutation

In order to evaluate the consequences of the *GPD1* mutation found in affected individuals, we cloned both wild-type and mutant *GPD1* cDNA, transfected HepG2 cells, and measured intracellular concentrations of cholesterol and TG as well as TG secretion into supernatant by HepG2 cells. By overexpressing either the mutant or wild-type allele, we simulated the homozygous recessive state in vivo. Overexpression of mutant *GPD1* in a human hepatocellular carcinoma-derived HepG2 cell line resulted in increased secretion of TG into the medium (~33%) compared to cells overexpressing the wild-type *GPD1* (Figure 5) (1.27 nM/mg protein versus 0.96 nM/mg protein, $p = 0.01$). Intracellular TG and cholesterol levels were also higher (~10% and ~20%) in cells overexpressing mutant *GPD1*; however, these changes did not reach statistical significance (Figure 5) ($p = 0.2$ and 0.7, respectively).

Discussion

In this study we show that a mutation in *GPD1* is associated with moderate to severe transient hypertriglyceridemia in infancy and early childhood that normalizes with age. The presence of an identical mutation in several families originating from the same village supports the presence of a founder effect in this isolated population. This is not surprising because the consanguinity rate within this specific population is high and affected individuals belong to only three large interrelated clans. The hypertriglyceridemia is associated with hepatomegaly and moderately elevated transaminases that may decrease later in life, persistent fatty liver, and the development of hepatic fibrosis. Serum TG levels are variable and could normalize during childhood or through adolescence.

The availability of G3P has been considered a possible regulatory factor in the synthesis of TGs.[30] It has been shown that the level of G3P in isolated hepatocytes from starved rats and glycogen-depleted hepatocytes from fed rats was low and severely limited TG synthesis. Raising the G3P level by the addition of precursors resulted in a hyperbolic-like relationship between TG synthesis and the cellular G3P level.[30] Despite the essential role of the enzyme in carbohydrate and lipid metabolism, no human diseases have yet been reported to be caused by mutations in *GPD1*.

The G3P shuttle is used to rapidly regenerate NAD^+ in the brain and skeletal muscle of mammals. Once G3P has passed through the inner mitochondrial membrane, it can be oxidized by a separate isoform of glycerol-3-phosphate dehydrogenase encoded by *GPD2*. Mitochondrial GPD2 is located on the outer surface of the inner

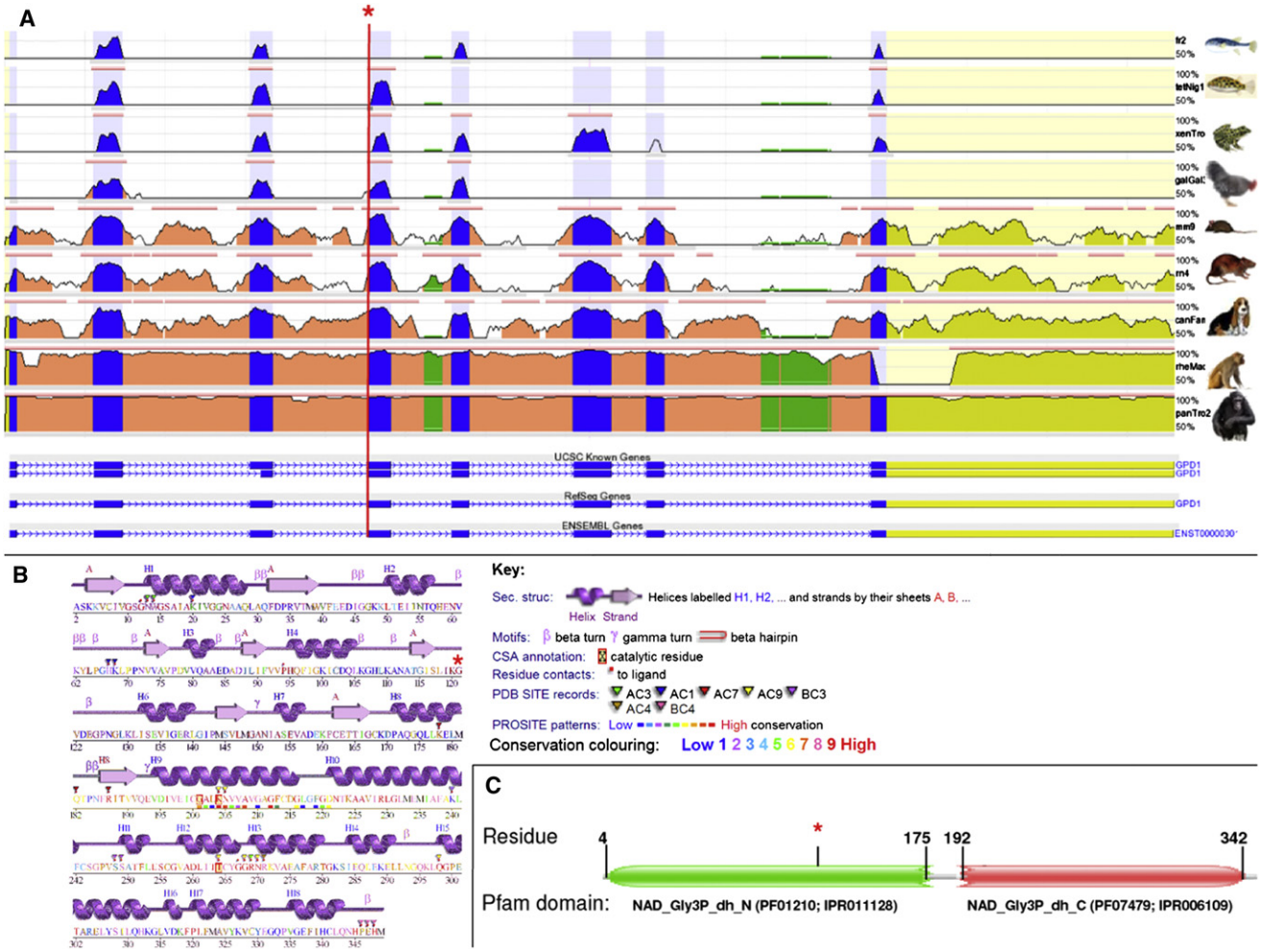

Figure 4. *GPD1* Gene Evolutionary Conservation and Protein Structure
(A) *GPD1* gene evolutionary conservation presented by ECR browser. Sequence conservation of exons (blue) and introns (orange), as well as UTR (yellow) and repeats (green) can be visualized. Layer height presents % identity of sequence pairwise alignment, asterisk and red vertical line represent the location of the mutation.
(B) Protein "wiring diagram" of GPD1. This schematic plot provides sequence, secondary structure elements, domains and motifs. The splicing point is marked on the protein's secondary structure (red asterisk). The protein sequence is colored by conservation (high sequence conservation is marked in red, low conservation in blue). Secondary structures (helices (H1-H18) and strands) are marked in purple. Legend key presents motifs, patterns and active sites (colored triangles) on the protein.
(C) GPD1 Domains. Two GPD1 Domains from Pfam are shown. The mutation is marked by a red asterisk.

mitochondrial membrane and catalyzes the unidirectional conversion of G3P to DHAP with concomitant reduction of the enzyme-bound FAD. Together with a cytosolic GPD1, GPD2 forms the glycerol phosphate shuttle, which uses the interconversion of G3P and DHAP to transfer reducing equivalents into mitochondria, resulting in the reoxidation of NADH formed during glycolysis. It is unknown whether mitochondrial NADH can drive lipid synthesis. Nevertheless, it should be mentioned that the affected individuals whom we studied show no clinical or laboratory evidence of mitochondrial disease or muscular weakness.

In our study we show that a mutation in *GPD1* leads to severe but transient hypertriglyceridemia, possibly by limiting the conversion of G3P to DHAP, and thus causing an increase in the amount of hepatic G3P available for TG synthesis. Alternatively, another intriguing theory is that because under physiological conditions GPD1 is oriented toward the conversion of DHAP to G3P, it is possible that accumulation of DHAP could lead to the overproduction of methylglyoxal, an alpha-ketoaldehyde and dicarbonyl,[31] which can behave as a highly toxic compound at the cellular level and which has been associated with renal fibrosis in diabetic patients.[32]

The transient nature of the hypertriglyceridemia in the individuals described in this study is compatible with the fact that the rates of TG secretion by hepatocytes are higher in neonates than in adults, as shown by Waterman et al.[33] in hepatocytes from rat livers of different ages. In addition, hepatic TG concentrations in rat liver are known to increase rapidly within the first 24 hr after birth and to decrease to adult values by the 10 days of age, whereas

Table 3. *GPD1* Variants Detected in Canadian Affected Individuals

Variant Name	Allele Frequency		
	Pediatric Hyperchylomicronemia (N = 16)	Adult Severe Hypertriglyceridemia (n = 75)	Adult Controls (n = 47)
Intron 1 +43C>G (ss475871079) (NM_005276.2:c.74+43C>G)	0.0	0.007	0.0
Intron 2 +20G>A (ss475871080) (NM_005276.2:c.252+20G>A)	0.0	0.0	0.011
p.I54V (rs2232202) (NM_005276.2:c.193A>G)	0.032	0.0	0.0
Intron 3 −114G>A (rs2232203) (NM_005276.2:c.394-114G>A)	0.0	0.027	0.064
Intron 3 −73G>A (rs2232204) (NM_005276.2:c.394-73G>A)	0.0	0.040	0.064
Intron 3 −56G>A (rs2232205) (NM_005276.2:c.394-56G>A)	0.0	0.040	0.021
p.E124K (rs34783513) (NM_005276.2:c.403G>A)	0.0	0.007	0.011
p.V197A (rs2232207) (NM_005276.2:c.623T>C)	0.032	0.0	0.0
p.K204K (rs35256655) (NM_005276.2:c.645G>A)	0.0	0.007	0.0
p.V206V (ss475871081) (NM_005276.2:c.651A>T)	0.0	0.007	0.0
p.T223I (ss475871082) (NM_005276.2:c.701C>T)	0.0	0.0	0.011
p.A225A (ss475871083) (NM_005276.2:c.708G>A)	0.0	0.0	0.011
p.A278A (ss475871084) (NM_005276.2:c.867G>A)	0.0	0.007	0.0
Intron 6 +10G>A (ss475871085) (NM_005276.2:c.879+10G>A)	0.0	0.0	0.011
p.I339I (rs836180) (NM_005276.2:c.1050C>T)	0.219	0.380	0.361
3′UTR +99C>T (ss475871086) (NM_005276.2:c.1083+99G>A)	0.0	0.007	0.0

plasma TG concentration is low in the newborn rat and rises rapidly to reach a peak value by 9 days of age, and there are no further changes until 21 days.[34] After weaning, the rat plasma TG concentration decreases gradually. The decrease in plasma TG concentration after several months of age in the individuals described here may be consistent with the observations in rats, although changes in dietary intake are another possible explanation.

gpd1 delta mutants in *Saccharomyces cerevisiae* produce very little glycerol, and they are sensitive to osmotic stress.[35] Mice showing loss of glycerol-3-phosphate dehydrogenase activity in adult tissues have normal morphological, physiological, and reproductive characteristics,[36] but in mice carrying ~25 copies of *Gpd1*, the amount of brown fat is greater than that in nontransgenic littermate controls. Glycerol 3-phosphate dehydrogenase activity in adipose tissue from morbidly obese subjects is approximately twice as high as it is in that from lean individuals.[37] Moreover, a positive correlation between adipose tissue glycerol 3-phosphate dehydrogenase activity and body mass index has been found. These data indicate that elevated glycerol 3-phosphate dehydrogenase might contribute to the increase of TG synthesis in obese subjects. In this study we show that, on the contrary, defective GPD1 activity causes severe hypertriglyceridemia leading to fatty liver. It is of note that the affected individuals described in this study have normal body mass indices, refuting the role of obesity in the pathophysiology of the development of hepatic steatosis in these individuals.

Our findings in HepG2 cells support the observation that the mutation causes increased TG synthesis and secretion levels. This in itself may explain the development of increased plasma TG levels, as well as fatty liver, in affected individuals, though other mechanisms related to the role of the enzyme in glyceroneogenesis[38] or oxidative phosphorylation could play a role in liver fat accumulation.

The pathophysiology of hepatosteatosis is not clear but could involve increased influx of fatty acids into the liver, decreased TG export from the liver, and impaired hepatic beta-oxidation and cellular energy homeostasis. Indeed, multiple factors may play substantial roles simultaneously. The molecular mechanisms that link steatosis to fibrosis and cirrhosis have yet to be clearly delineated. Nonalcoholic fatty liver disease (NAFLD) is usually related to diabetes mellitus, obesity, and hyperlipidemia and is the hepatic component of the metabolic syndrome.[39] It is also part of other lipid disorders (abetalipoproteinemia), infectious diseases (hepatitis C), disorders involving carbohydrate metabolism (glycogen storage diseases, hereditary fructose intolerance, galactosemia), protein metabolism (homocystinuria, tyrosinemia), as well as disorders of the mitochondria and oxidative phosphorylation.[40] Although NAFLD can be a relatively benign disease in many affected individuals, cirrhosis might develop in 20% of those affected.[39] Thus the development of hepatic fibrosis in affected individuals might be the result of the fat accumulation in liver tissue. However, specific triggers related to

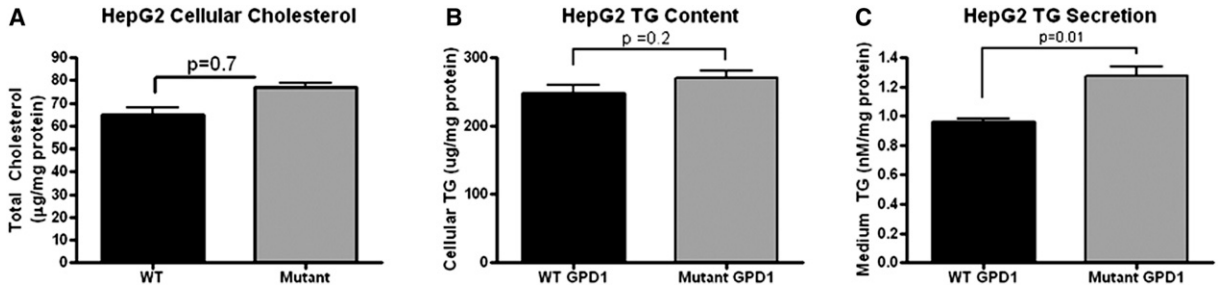

Figure 5. Intracellular and Secreted TG and Total Cholesterol Concentration in HepG2 Cells Overexpressing Wild-Type and Mutant *GPD1* cDNA

(A) Total cholesterol content in wild-type and mutant *GPD1* overexpressing Hep2G cells.
(B) TG content in wild-type and mutant *GPD1* overexpressing HepG2 cells.
(C) TG accumulation in medium in wild-type and mutant GPD1 overexpressing HepG2 cells.
Error bars represent standard error of the mean.

the mutation in *GPD1* cannot be excluded and will need to be sought in the future.

It is important to emphasize that no clinical evidence of coronary heart disease or episodes of recurrent pancreatitis have been observed in the oldest individual (aged 23 years). However, most affected individuals evaluated in this study are young, and no conclusions can be drawn at this point about the influence of severe childhood hypertriglyceridemia on the risk for coronary heart disease or about the effect of this mutation on longevity. Heterozygous family members do not have recorded increased TG levels or hepatomegaly in childhood, nor do they have biochemical evidence of hepatic dysfunction. Long-term follow-up of both affected individuals and heterozygotes will help to clarify the issue of any long-term morbidity associated with the mutation.

In summary, we have demonstrated that a *GPD1* mutation may be responsible for moderate to severe hypertriglyceridemia and fatty liver in early infancy followed by reduction and even normalization of TG serum levels later in life, but with sustained liver dysfunction and progression of the fatty liver to fibrosis.

Supplemental Data

Supplemental Data includes one table and can be found with this article online at http://www.cell.com/AJHG/.

Acknowledgments

The authors thank Gabrielle J. Halpern for her help with editing the manuscript, Hava Fleischaker for her help with the multiple tests these families underwent, and the families for their participation. R.A.H. is supported by operating grants from the Canadian Institutes for Health Research (MOP-13430, MOP-79523, CTP-79853), the Heart and Stroke Foundation of Ontario (NA-6059, T-6018, PRG-4854), and Genome Canada through the Ontario Genomics Institute. L.G., S.P., and E.A.F. were supported by National Institute of Health grant HL58541. This study was supported by the Adler Chair in Pediatric Cardiology, Tel Aviv University.

Received: September 1, 2011
Revised: November 16, 2011
Accepted: November 29, 2011
Published online: January 5, 2012

Web Resources

The URLs for data presented herein are as follows:

Bgee database, http://bgee.unil.ch/bgee/bgee
CDC 2000, https://www.cdc.gov/growthcharts
ECR (Evolutionary Conserved Regions) browser, http://ecrbrowser.dcode.org
Homozygosity Mapper program, http://www.homozygositymapper.org
InterPro server (IPR), http://www.ebi.ac.uk/interpro/
London Regional Genomics Centre, ON, www.lrgc.ca
Online Mendelian Inheritance in Man (OMIM), http://www.omim.org/
Pfam database (PF) version 24.0 (10/2009), http://pfam.janelia.org/
Primer3 program, http://frodo.wi.mit.edu/primer3/
UCSC Genome Browser (assembly hg19), http://genome.ucsc.edu/
UniProt server, http://www.uniprot.org/

References

1. Cohen, H., and Shamir, R. (2007). Lipid disorders in children and adolescents. In Pediatric Endocrinology, Fifth Edition, F. Lifshitz, ed. (New York: Informa Healthcare), pp. 279–290.
2. Merkel, M., Eckel, R.H., and Goldberg, I.J. (2002). Lipoprotein lipase: Genetics, lipid uptake, and regulation. J. Lipid Res. *43*, 1997–2006.
3. Yuan, G., Al-Shali, K.Z., and Hegele, R.A. (2007). Hypertriglyceridemia: Its etiology, effects and treatment. CMAJ *176*, 1113–1120.
4. Boyd, G.S., Koenigsberg, J., Falkner, B., Gidding, S., and Hassink, S. (2005). Effect of obesity and high blood pressure on plasma lipid levels in children and adolescents. Pediatrics *116*, 442–446.
5. Garcés, C., Gutierrez-Guisado, J., Benavente, M., Cano, B., Viturro, E., Ortega, H., and de Oya, M. (2005). Obesity in Spanish schoolchildren: Relationship with lipid profile and insulin resistance. Obes. Res. *13*, 959–963.

6. Jacobs, M.J., Kleisli, T., Pio, J.R., Malik, S., L'Italien, G.J., Chen, R.S., and Wong, N.D. (2005). Prevalence and control of dyslipidemia among persons with diabetes in the United States. Diabetes Res. Clin. Pract. *70*, 263–269.
7. Lai, S.W., Ng, K.C., Lin, H.F., and Chen, H.L. (2001). Association between obesity and hyperlipidemia among children. Yale J. Biol. Med. *74*, 205–210.
8. Reinehr, T., Andler, W., Denzer, C., Siegried, W., Mayer, H., and Wabitsch, M. (2005). Cardiovascular risk factors in overweight German children and adolescents: Relation to gender, age and degree of overweight. Nutr. Metab. Cardiovasc. Dis. *15*, 181–187.
9. Sherry, N., Hassoun, A., Oberfield, S.E., Manibo, A.M., Chin, D., Balachandar, S., Pierorazio, P., Levine, L.S., and Fennoy, I. (2005). Clinical and metabolic characteristics of an obese, Dominican, pediatric population. J. Pediatr. Endocrinol. Metab. *18*, 1063–1071.
10. Hegele, R.A. (2009). Plasma lipoproteins: Genetic influences and clinical implications. Nat. Rev. Genet. *10*, 109–121.
11. Bishop, J.R., Passos-Bueno, M.R., Fong, L., Stanford, K.I., Gonzales, J.C., Yeh, E., Young, S.G., Bensadoun, A., Witztum, J.L., Esko, J.D., and Moulton, K.S. (2010). Deletion of the basement membrane heparan sulfate proteoglycan type XVIII collagen causes hypertriglyceridemia in mice and humans. PLoS ONE *5*, e13919.
12. Celermajer, D.S., Sorensen, K.E., Gooch, V.M., Spiegelhalter, D.J., Miller, O.I., Sullivan, I.D., Lloyd, J.K., and Deanfield, J.E. (1992). Non-invasive detection of endothelial dysfunction in children and adults at risk of atherosclerosis. Lancet *340*, 1111–1115.
13. Tonstad, S., Joakimsen, O., Stensland-Bugge, E., Leren, T.P., Ose, L., Russell, D., and Bønaa, K.H. (1996). Risk factors related to carotid intima-media thickness and plaque in children with familial hypercholesterolemia and control subjects. Arterioscler. Thromb. Vasc. Biol. *16*, 984–991.
14. Assmann, G., Cullen, P., and Schulte, H. (1998). The Münster Heart Study (PROCAM). Results of follow-up at 8 years. Eur. Heart J. *19* (*Suppl A*), A2–A11.
15. Criqui, M.H., Heiss, G., Cohn, R., Cowan, L.D., Suchindran, C.M., Bangdiwala, S., Kritchevsky, S., Jacobs, D.R., Jr., O'Grady, H.K., and Davis, C.E. (1993). Plasma triglyceride level and mortality from coronary heart disease. N. Engl. J. Med. *328*, 1220–1225.
16. Cullen, P. (2000). Evidence that triglycerides are an independent coronary heart disease risk factor. Am. J. Cardiol. *86*, 943–949.
17. Hokanson, J.E., and Austin, M.A. (1996). Plasma triglyceride level is a risk factor for cardiovascular disease independent of high-density lipoprotein cholesterol level: A meta-analysis of population-based prospective studies. J. Cardiovasc. Risk *3*, 213–219.
18. Hopkins, P.N., Wu, L.L., Hunt, S.C., and Brinton, E.A. (2005). Plasma triglycerides and type III hyperlipidemia are independently associated with premature familial coronary artery disease. J. Am. Coll. Cardiol. *45*, 1003–1012.
19. Athyros, V.G., Giouleme, O.I., Nikolaidis, N.L., Vasiliadis, T.V., Bouloukos, V.I., Kontopoulos, A.G., and Eugenidis, N.P. (2002). Long-term follow-up of patients with acute hypertriglyceridemia-induced pancreatitis. J. Clin. Gastroenterol. *34*, 472–475.
20. Seelow, D., Schuelke, M., Hildebrandt, F., and Nürnberg, P. (2009). HomozygosityMapper – an interactive approach to homozygosity mapping. Nucleic Acids Res. *37* (Web Server issue), W593–W599.
21. Johansen, C.T., Wang, J., Lanktree, M.B., Cao, H., McIntyre, A.D., Ban, M.R., Martins, R.A., Kennedy, B.A., Hassell, R.G., Visser, M.E., et al. (2010). Excess of rare variants in genes identified by genome-wide association study of hypertriglyceridemia. Nat. Genet. *42*, 684–687.
22. Ovcharenko, I., Nobrega, M.A., Loots, G.G., and Stubbs, L. (2004). ECR Browser: A tool for visualizing and accessing data from comparisons of multiple vertebrate genomes. Nucleic Acids Res. *32* (Web Server issue), W280–W286.
23. Laskowski, R.A. (2001). PDBsum: Summaries and analyses of PDB structures. Nucleic Acids Res. *29*, 221–222.
24. Ou, X., Ji, C., Han, X., Zhao, X., Li, X., Mao, Y., Wong, L.L., Bartlam, M., and Rao, Z. (2006). Crystal structures of human glycerol 3-phosphate dehydrogenase 1 (GPD1). J. Mol. Biol. *357*, 858–869.
25. Finn, R.D., Mistry, J., Tate, J., Coggill, P., Heger, A., Pollington, J.E., Gavin, O.L., Gunasekaran, P., Ceric, G., Forslund, K., et al. (2010). The Pfam protein families database. Nucleic Acids Res. ***38*** (Database Issue), D211–D222.
26. Hunter, S., Apweiler, R., Attwood, T.K., Bairoch, A., Bateman, A., Binns, D., Bork, P., Das, U., Daugherty, L., Duquenne, L., et al. (2009). InterPro: The integrative protein signature database. Nucleic Acids Res. ***37*** (Database Issue), D211–D215.
27. Bastian, F., Parmentier, G., Roux, J., Moretti, S., Laudet, V., and Robinson-Rechavi, M. (2008). Bgee: Integrating and comparing heterogeneous transcriptome data among species. Lect. Notes Comput. Sci. *5109*, 124–131.
28. Menaya, J., González-Manchón, C., Parrilla, R., and Ayuso, M.S. (1995). Molecular cloning, sequencing and expression of a cDNA encoding a human liver NAD-dependent alpha-glycerol-3-phosphate dehydrogenase. Biochim. Biophys. Acta *1262*, 91–94.
29. Gao, Y.Z., Jiang, Y., Wu, X., Bai, C.Y., Pan, Y.C., and Sun, Y.Z. (2011). Molecular characteristics and expression profiles of glycerol-3-phosphate dehydrogenase 1 (GPD1) gene in pig. Mol. Biol. Rep. *38*, 1875–1881.
30. Declercq, P.E., Debeer, L.J., and Mannaerts, G.P. (1982). Role of glycerol 3-phosphate and glycerophosphate acyltransferase in the nutritional control of hepatic triacylglycerol synthesis. Biochem. J. *204*, 247–256.
31. Chaplen, F.W., Fahl, W.E., and Cameron, D.C. (1998). Evidence of high levels of methylglyoxal in cultured Chinese hamster ovary cells. Proc. Natl. Acad. Sci. USA *95*, 5533–5538.
32. Ho, C., Lee, P.H., Huang, W.J., Hsu, Y.C., Lin, C.L., and Wang, J.Y. (2007). Methylglyoxal-induced fibronectin gene expression through Ras-mediated NADPH oxidase activation in renal mesangial cells. Nephrology (Carlton) *12*, 348–356.
33. Waterman, I.J., Price, N.T., and Zammit, V.A. (2002). Distinct ontogenic patterns of overt and latent DGAT activities of rat liver microsomes. J. Lipid Res. *43*, 1555–1562.
34. Jamdar, S.C., Moon, M., Bow, S., and Fallon, H.J. (1978). Hepatic lipid metabolism. Age-related changes in triglyceride metabolism. J. Lipid Res. *19*, 763–770.
35. Albertyn, J., Hohmann, S., Thevelein, J.M., and Prior, B.A. (1994). GPD1, which encodes glycerol-3-phosphate dehydrogenase, is essential for growth under osmotic stress in Saccharomyces cerevisiae, and its expression is regulated by the high-osmolarity glycerol response pathway. Mol. Cell. Biol. *14*, 4135–4144.

36. Prochazka, M., Kozak, U.C., and Kozak, L.P. (1989). A glycerol-3-phosphate dehydrogenase null mutant in BALB/cHeA mice. J. Biol. Chem. *264*, 4679–4683.
37. Swierczynski, J., Zabrocka, L., Goyke, E., Raczynska, S., Adamonis, W., and Sledzinski, Z. (2003). Enhanced glycerol 3-phosphate dehydrogenase activity in adipose tissue of obese humans. Mol. Cell. Biochem. *254*, 55–59.
38. Reshef, L., Olswang, Y., Cassuto, H., Blum, B., Croniger, C.M., Kalhan, S.C., Tilghman, S.M., and Hanson, R.W. (2003). Glyceroneogenesis and the triglyceride/fatty acid cycle. J. Biol. Chem. *278*, 30413–30416.
39. Reid, A.E. (2010). Non alcoholic fatty liver disease. In Sleisenger and Fordtran's Gastrointestinal and Liver Disease, Ninth Edition, M. Feldman, L.S. Friedman, and L.J. Brandt, eds. (Philadelphia: Elsevier), pp. 1401–1411.
40. Lee, W.S., and Sokol, R.J. (2007). Mitochondrial hepatopathies: advances in genetics and pathogenesis. Hepatology *45*, 1555–1565.